Orthopositronium study of positron-irradiation-induced surface defects in alumina powder

C. Dauwe
Laboratorium voor Magnetisme, Rijksuniversiteit Gent, Proeftuinstraat 86, 9000 Gent, Belgium

Mbungu-Tsumbu
Département de Physique, Université de Kinshasa, Boîte Postale 190 KIN XI, Zaire
(Received 26 December 1990; revised manuscript received 23 April 1991)

Three-quantum-yield measurements and orthopositronium (*o*-Ps)-lifetime spectrometry at low temperatures are used to study the interaction of positronium with the surface in fine powders of aluminum oxide. It is found that electron and/or positron irradiation of the specimen induces surface defects which influence the positronium in three ways: (1) A surface positroniumlike bound state is created, (2) the fraction of *o*-Ps escaping from the particles is slightly inhibited, and (3) the escaped *o*-Ps is quenched into two-quantum decay upon collisions with the surface defects. It is found that the surface Ps state is not populated at the expense of the interparticle Ps. The most likely surface defects are Al^{2+} or Al^{0} due to the migration of irradiation-induced interstitials. The techniques of long-lifetime spectrometry and of three-quantum-annihilation-rate measurement could be used to study both the diffusion of bulk defects to the surfaces, and the interactions of *o*-Ps to surface defects.

I. INTRODUCTION

Positron annihilation in fine powdered materials is an increasingly interesting subject for its fundamental aspects and for its potential technical and industrial applications. In pure metal powders the injected positrons annihilate in the inside as free bulk positrons, or diffuse to the surface where some emerge as hot positrons[1] with an energy corresponding to the negative positron work function. Others may be trapped in a surface state from which they boil off at high temperatures as epithermal positrons[2] or as positronium (Ps). The situation is rather more complicated in the case of fine powdered insulator oxides such as SiO_2, Al_2O_3, and MgO,[3] which show very long-lifetime components and high three-quantum yields due to the formation of free orthopositronium (*o*-Ps) in the interparticle space. The common idea is that perturbed positronium, or quasipositronium (qPs), is formed both in the para- and in the orthostate inside of the oxide particles, diffuses to the surface and eventually is ejected with an energy that depends on the positronium work function[4] and on the positronium effective temperature which itself depends on the efficiency of the thermalization process and on the implantation depth.[5] In fine particles the implantation depth can never be greater than the particle radius and all the positrons are effectively implanted near the surface, which means that no appreciable thermalization of the Ps takes place after its formation and before ejection. This lack of thermalization of the Ps is the reason why the cooling of a powder specimen to 20 K has no immediate effect on the diffusion constant and on the amount of interparticle *o*-Ps.[6] For a number of ionic or mixed ionic-covalent materials the formation of qPs in the bulk has not been clearly established and it may be argued that the thermalized positron itself diffuses to the surface and escapes, whereby it may be energetically favorable to associate with a surface electron and to escape as a positronium atom. The question of preexistence of bulk qPs can only be settled by one of two methods: (1) the observation of a narrow parapositronium peak in the annihilation angular correlation (PAC) of the corresponding single crystals and (2) the observation of magnetic quenching either of lifetime components or of the three-quantum annihilation rate. Thus positronium definitely exists in well-crystallized ice,[7] quartz,[8] MgF_2,[9] CaF_2,[10] and the alkali halides,[11] while the question is still unsettled for Al_2O_3 and MgO.

Other metal oxide powders such as Fe_2O_3 (Ref. 12) and ThO_2 (Ref. 13) show no sign of free interparticle *o*-Ps, even at very small particle sizes. Graphite behaves like metal powder in the sense that the surface is a trap for positrons and that the interparticle Ps, if any exists, is very strongly quenched.[14]

The unsettled question of existence of positronium in the bulk of Al_2O_3 is crucial to this work; on the one hand, positronium has never been clearly detected in well-crystallized Al_2O_3, but on the other hand, many authors accept the formation of positronium inside alumina fine particles. Lifetime experiments in bulk Al_2O_3 distinguish only two components, one at (140±10) ps due to free positrons, and a second one at (165±5) ps accepted to correspond to positrons trapped in aluminum vacancies.[15] If both views are to be accepted then fine particles are fundamentally different from bulk material. In this work we will accept as a working hypothesis[16] that positronium is formed inside alumina fine particles and diffuses to the surface eventually to be ejected.

After escaping, interparticle *o*-Ps can lower its excess energy only through collisions with the particle surface or with rest gases filling the space. Experimental and theoretical[17] evidence show that the interaction of Ps to the perfect surface is mainly by elastic collisions and that the *o*-Ps loses only a small fraction of its excess energy during its lifespan. Thus, in the case of high vacuum and perfect powder surfaces the *o*-Ps decay is one of nearly free hot Ps with a lifetime which is very close to the natu-

ral decay lifetime of 142 ns.

The situation can change drastically in two cases: (1) when the surface contains any form of quenching defect, such as adsorbed atoms, free radicals, paramagnetic centers, etc., and (2) when the free space is filled with gases. At high temperature we may ignore the physisorbed surface layer of the fill gas which means that the quenching of the *o*-Ps is due to the scattering on the gas molecules. Experiments on the *o*-Ps to oxygen gas interaction in SiO_2 powders show that the cross section for inelastic scattering and thermalization is three orders of magnitude higher than the cross section for elastic scattering. Both the oxygen molecule and the positronium atom have an ortho- and parastate and the inelastic scattering results in a very efficient *o-p-o* conversion.[18] The halide gas bromine is still a thousand times more efficient as an *o*-Ps quencher than oxygen because of the chemical affinity of Ps to the halides.[19] In the absence of fill gases the Ps-surface quenching shows that in fact the quenching is due to surface defects and that it is possible to screen these surface defects with a monomolecular layer of adsorbed noble gases such as helium. This monomolecular antiquenching effect of He on SiO_2 particles has been demonstrated by Kiefl and Harshman,[20] who found that the amount of observed Ps reached its maximum value at the monolayer covering. The same antiquenching of *o*-Ps effect was observed by Rice-Evans *et al.*[21] for the helium and nitrogen covering of graphite. These authors also found a puzzling increase of parapositronium annihilation in graphite due to the adsorption of oxygen between 80 and 160 K.[22]

The behavior of muonium formed in the free space around Al_2O_3 grains confirms the capital importance of defects on the surface; when the surface is screened by means of the adsorption of a submonomolecular layer of helium, the spin relaxation rate of this muonium is proportional to the fraction of the surface which is not covered by helium.[23]

In previous work[6] we have presented the results of *o*-Ps yield measurements in fine powdered Al_2O_3 by means of three-quantum annihilation. The specimen was placed with a ^{68}Ge positron source of 10.8 μCi in an open ended tube and was evacuated to 10^{-5} mbar before cooling to $\sim$20 K. In these conditions we should observe a nearly free *o*-Ps natural decay having little or no interaction to the surface of the particles, and thus the three-quantum count rate should be unaffected by the cooling of the sample. Surprisingly the three-quantum isotherms showed a time-dependent decrease of the count rate but we did not observe a matching change in the lifetime experiments which were obtained with a highly efficient CsF spectrometer where the positron source was ^{22}Na of 0.22 μCi, i.e., 50 times weaker than the three-quantum source. In this paper we show that the apparent paradox is easily lifted when equivalent-strength positron sources are used and that the observed effects can be used as a method for the study of irradiation-induced surface defects.

II. EQUIPMENT AND SAMPLES

For this work we used two lifetime spectrometers and one triple-coincidence apparatus, which has been described in full detail elsewhere.[24] The triple-coincidence count rate was registered by a microcomputer-based multiscaler, with a counting time per channel set at 30 min. The count rate is typically 20 s^{-1} for a 0.05-μm mean diameter alumina powder sample with the ^{68}Ge source. For the short component lifetimes we used the University of Kinshasa fast-fast spectrometer equipped with two 3-cm diam by 2.5-cm height BaF_2 crystals mounted on XP2020Q phototubes, with timing signals derived from the 9th dynode. The overall time resolution full width at half maximum (FWHM) was 215 ps as is determined from the fitting of the resolution function in real spectra. For these lifetime experiments and for the three-quantum experiments the sample could be evacuated and cooled in a closed-cycle helium-gas refrigerator which allowed temperatures as low as 20 K with a temperature stability of 0.5 K. The long or free *o*-Ps lifetimes have been measured with a similar BaF_2 spectrometer at the Ghent State University. In this case the timing resolution is less critical and the stop channel energy selection was set at $\sim$300 keV in order to enhance the three-quantum lifetime detection efficiency. In this case cooling was limited at 77 K since all necessary data could be obtained at this temperature. A number of different positron and electron sources were used as is shown in Table I. The ^{68}Ge sources are fundamental for good three-quantum measurements because they emit almost no coincident nuclear γ ray; the ^{204}Tl electron source emits no γ ray at all and is intended to increase the defect production without raising the perturbing γ background, and the ^{22}Na sources are ubiquitous for lifetime measurements.

The aluminum oxide powders are Linde grade A, B,

TABLE I. Characteristics of the positron and electron sources.

Code	Isotope	Activity (μCi)	E_β (keV)	Support	Application	Laboratory
S1	^{68}Ge	10.8±0.4	1880	Ni foil	3-γ isotherms	Kinshasa
S2	^{68}Ge	7.6,6.6[a]	1880	Ni foil	3-γ isotherms	Kinshasa
S3	^{204}Tl	5.5±0.1	763	Kapton	3-γ isotherms	Kinshasa
S4	^{204}Tl	16.5±0.3	763	Kapton	3-γ isotherms	Kinshasa
S5	^{204}Tl	38.5±0.7	763	Kapton	3-γ isotherms	Kinshasa
S6	^{22}Na	6.3±0.3	545	Kapton	Short τ and 3-γ	Kinshasa
S7	^{22}Na	10±3	545	Kapton	Long τ	Ghent
S8	^{22}Na	20±6	545	Kapton	Long τ	Ghent

[a]The two values indicate the decay of the source over the period of the three-quantum isotherm measurements.

TABLE II. Characteristics of the analyzed powder specimen.

Code	Material	Part. Diameter (μm)	Hardness (Moh)	Lattice
P1	γ-Al_2O_3	0.05	8	Cubic
P2	α-Al_2O_3	0.3	9	Hexagonal
P3	α-Al_2O_3	1.0	9	Hexagonal

and C micropolishing powders, obtained from Buehler Ltd. (Illinois), of 99.98+ % chemical purity. According to the specifications of the manufacturer the principal impurities are Na (5–40 pps), Pb (40 ppm), Si (50 ppm), Fe (10 ppm), Ca (2 ppm), and Mg (2 ppm). The other properties of the alumina powders we used are shown in Table II. γ-alumina is known to have a partially hydrated surface for which a model has been described by Peri[25] who distinguishes five types of surface hydroxyl ions which are associated with five infrared absorption bands between 3700 and 3800 cm^{-1}, and also a number of possible surface defects thought to be responsible for the catalytic properties. Our samples were initially kept in vacuum for a few hours at 50 °C and no further specific treatment was given, which means that they certainly contain a number of surface hydroxyl ions, water molecules, and/or defects. As we mentioned in our early paper the measured free o-Ps lifetime at 300 K is (135±2) ns, which is slightly lower than the theoretical value of 142 ns. Following Gidley, Marko, and Rich[26] this o-Ps lifetime depends on an effective density ρ^* which is a mean over the free space and the space occupied by the powder particles, and the o-Ps lifetime approaches the theoretical value of 142 ns when $\rho^* \rightarrow 0$. Thus it is clear that this lowering of the o-Ps lifetime at room temperature is due to its interaction to the particle surfaces, most probably the surface hydroxyl ions.

III. EXPERIMENTAL RESULTS AND INTERPRETATION

A. Long-lifetime isotherm and the interparticle free orthopositronium

In order to observe the evolution of the interparticle free o-Ps formation fraction $P_F(T,t)$ and its lifetime τ_F we used the BaF_2 lifetime spectrometer at the Ghent State University with a time scale setting of 2 ns/channel. Two positron sources S7 and S8 were used, and the stop-channel energy selection was set to accept all energies, i.e., $50 < E < 600$ keV. After evacuation at room-temperature (RT) for 24 h the specimen was cooled to 77 K and consecutive lifetime spectra were accumulated during 2 h each. In this mode all short components are compressed into a few channels around zero time and the analyzable tail contains one long component and a constant background. Figure 1 shows the o-Ps lifetime and its relative intensity as functions of cooling time in the 0.05-μm powder P1. It is seen that upon cooling to 77 K both the free o-Ps lifetime τ_F and its relative intensity $I^F_{o\text{-Ps}}$ decrease and it is clear that the double strength source S8 causes a much stronger effect than source S7, which is a strong indication for the defect production relatedness of these effects. These variations of τ_F and $I^F_{o\text{-Ps}}$ seems to contradict our own results[6] where no variation of these parameters could be discerned even after long cooling times to 25 K. The reason is that our 1989 results were obtained with a very high efficiency CsF spectrometer and that an extremely weak positron source of 0.22 μCi was used, thus the defect production rate was some 50–100 times lower than in the present experiments.

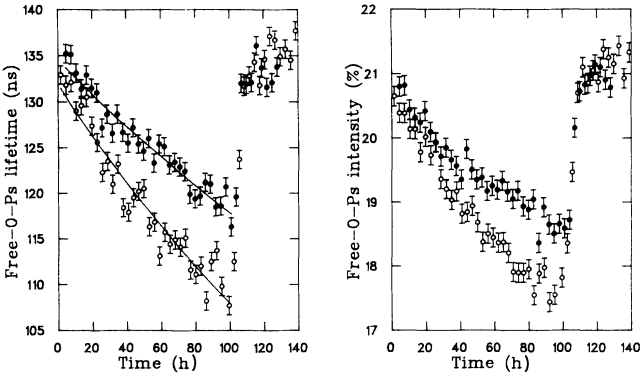

FIG. 1. Free-orthopositronium lifetime τ_F and relative intensity $I^F_{o\text{-Ps}}$ isotherms at 77 K for two ^{22}Na positron sources; (●) are for a 10-μCi source strength, (○) are for a 20-μCi source. After 100 h at 77 K the samples are allowed to warm to room temperature.

In order to interpret the real o-Ps fraction we have to consider that in long-lifetime spectrometry the free o-Ps decay is seen simultaneously through its two-quantum quenching channel and through its three-quantum natural decay channel as a single lifetime component, although each detection mode has its own detection efficiency, i.e., α_2 and α_3. The detailed description of the calibration procedure for the intensities of such mixed-mode components is the subject of a forthcoming paper[27] from which we retain the conclusion that the free orthopositronium fraction P_F and its experimental intensity $I^F_{o\text{-Ps}}$ are related by

$$I^F_{o\text{-Ps}} = \frac{1-\beta_F+\beta_F\eta(E)}{1/P_F-\beta_F+\beta_F\eta(E)}\ , \qquad \eta(E)=\frac{\alpha_3(E)}{\alpha_2(E)},\ \text{and}\ \beta_F=\frac{\tau_F}{\tau_0}=\frac{\lambda_0}{\lambda_0+\lambda_{qv}}\ , \tag{1}$$

where $\eta(E)$ is the stop-channel energy-dependent efficiency ratio. From such an analysis we obtained $\eta(50\text{–}600\ \text{keV})=(4.1\pm0.1)$, and $P_F(0)=(6.1\pm0.1)\%$ for the specimen P1.

Now we can use Eq. (1) with the known value of $\eta(50\text{–}600$ keV) to calculate the free o-Ps fraction as a function of cooling time at 77 K. This experimental fraction $P_F(77\ \text{K},t)$ splits in a natural way into two data sets, corresponding to the two source strengths. It is, however, interesting to represent $P_F(77\ \text{K},t)$ versus the relative quenching rate $\lambda_{qv}/\lambda_0=(\lambda_F-\lambda_0)/\lambda_0$. This relation is represented in Fig. 2 and we see a single linear decease of the formed o-Ps fraction, i.e., an inhibition which is proportional to the quenching rate and which can be represented by $P_F=0.061(1-0.17\lambda_{qv}/\lambda_0)$. In absolute

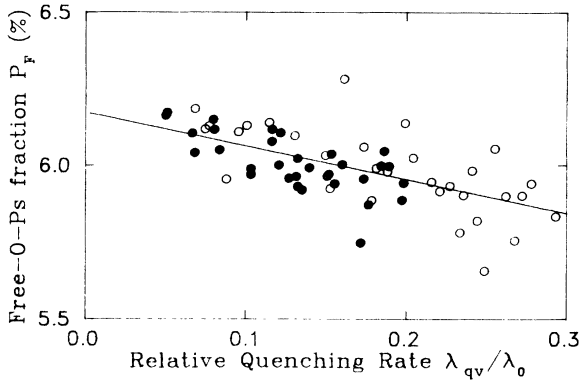

FIG. 2. Free o-Ps fraction P_F, calculated from the data in Fig. 1 using Eq. (1), vs quenching rate in γ-alumina fine powder. The data (●) are obtained with the 10-μCi source S7, the data (○) are from the double strength source S8.

terms this inhibition is rather weak, as for a lifetime reduction of 30% the corresponding o-Ps yield P_F changes only from 6.1% to 5.8%. It is interesting to note that the two phenomena, however, act at different moments; the inhibition occurs at the moment of ejection of the bulk positronium, while the quenching of the free positronium occurs at the collisions with the surface a mean time of 100 ns later. The quenching of free positronium is necessarily due to changes in the state of the particle surface, but the inhibition may have different interpretations.

(1) If no positronium is formed in aluminum oxide, the observed free positronium is generated by positrons which diffuse to the surface and pick up an electron to be ejected as positronium rather than as isolated positrons. These diffusing bulk positrons may be trapped into Al^{3+} vacancies created by the thermalization of energetic positrons. The trapping of positrons in electron-irradiation-induced cation vacancies was studied by Forster, Mundy, and Schaefer,[15] who observed saturation trapping of positrons in aluminum oxide irradiated with a dose of 1.3×10^{23} e^-/m^2. Unfortunately no observations at lower doses are known and we cannot predict the minimum dose for observable damage. In our experiment an approximate equivalent dose can be calculated from the source intensity; it is easily seen that with a 3-mm-diam source of 10 μCi the maximum possible dose received after 24 h by any part of the sample is $\approx2\times10^{15}$ e^-/m^2 which is eight orders of magnitude lower than the saturation dose used by Forster, Mundy, and Schaefer. Therefore we rule out trapping of positrons as an inhibition mechanism for the free positronium.

(2) If positronium is formed in the bulk of aluminum oxide the observed inhibition of free positronium might be due to at least two possible mechanisms: (i) Part of the positronium due to escape may be retained at the surface, in which case a surface positronium state should be populated with an amount equal to the inhibited part of the free positronium. As we will see in Sec. III B a surface orthopositronium state is indeed populated but its intensity easily attains 5–6 %, which is an order of magnitude higher than can be expected from the inhibited fraction. Thus a small part of the surface orthopositronium state may well be populated by the inhibition of the free orthopositronium. (ii) The bulk positronium might be trapped in radiation-induced defects, such as aluminum vacancies or oxygen vacancies. To our knowledge no indication exists in the literature for this trapping of positronium by single-vacancy-type defects in aluminum oxide or any other metal oxide.

B. Short-lifetime isotherms and the surface orthopositronium

A five detector setup at the University of Kinshasa, i.e., two BaF_2 for the timing and three NaI(Tl) for the triple coincidences, allowed almost simultaneous three-quantum and lifetime experiments with a ^{22}Na source S6. First a lifetime spectrum was obtained at room temperature; then the BaF_2 detectors are slightly withdrawn and the cooling to a preset temperature is started, which takes typically 45 min. The three-quantum count rate is now monitored for at least 50 h after which a few consecutive lifetime spectra are obtained. By extrapolation of the observed three-quantum isotherm we know he three-quantum count ratio $Q(T,t)=N_3(T,t)/N_3(0)$ at the mean time of obtaining the lifetime spectra. This procedure was followed for the 0.05-μm particle size specimen P1 and for the 0.3-μm particle size specimen P2; in the 1.0-μm specimen P3 the quantity of positrons reaching the surface is so small that the lifetime spectra are practically identical to the spectrum obtained from bulk aluminum oxide. A typical spectrum obtained with a time calibration of 25 ps/channel contains 10^6 total counts, a background of ≈10 counts/channel and a free o-Ps tail contribution of ≈30 counts at time zero, decreasing to ≈23 at the end of the region of interest. The source contribution should consist of a few percent of the Kapton support foil spectrum, which is single component at 382 ps, the intensity of which depends on the foil thickness and on the mean atomic weight of the specimen. It is general practice to determine this source component by fitting the intensity of an added lifetime component with fixed value at 382 ps; unfortunately the second component of the alumina spectrum has nearly the same value and therefore it is impossible to impose any constraints on lifetimes of this magnitude. As a result the obtained values for the second component are a mean of an intrinsic alumina component and of the source contribution. We have to point out that the short-component relative intensities are normalized to total two-quantum components $=100\%$, i.e., the three-quantum very long o-Ps component, with a maximum real fraction of $\approx6\%$ in P1, $\approx2\%$ in P2, and $<1\%$ in P3, is not considered here. The shortest obtained lifetime component τ_1 with a mean value of 141–152 ps has an intensity at RT which varies from 37% in sample P1 to 53% in P2 and finally to 76% in P3 while the intensity of the second component of $\tau_2\approx360$–432 ps varies inversely from 58% to 47% and 23%. This dependency of I_1 and I_2 on particle size is consistent with the assignment proposed by Brauer *et al.*[28] who identified the shortest component in alumina as a free-positron state in the perfect

lattice. We believe that this lifetime is mixed up with a weak parapositronium lifetime which has to be present with an intensity of one-third of the o-Ps fraction, i.e., it should have 2% of the total number of annihilations in the 0.05-μm powder spectra. The second component is assigned by Brauer *et al.* to a surface positron state. However, great care should be taken with this component for it is probably a mixture of three as yet indistinguishable components: (1) a surface positron state, (2) a bulk quasipositronium state, and (3) the source support foil component.

A third rather weak component is present in the smallest grain specimen P1. This component $(\tau_2', I_2') \approx (700$ ps, 5%) has not been observed by any other author and its signification is enigmatic as yet. As it has not been observed in the α-alumina powders P2 and P3 it might be associated with the structural vacancies which are characteristic of the γ phase of alumina. At low temperatures the really interesting feature of these lifetime isotherms is the appearance of a medium-long component τ_3 at (5 ± 1) ns with a relative intensity $I_3(T,t)$ which shows a linear relationship to $N_3(0)/N_3(T,t)=Q^{-1}(T,t)$, the inverse of the three-quantum count ratio, as we can see clearly from Fig. 3. The appearance of this component in the 0.05-μm sample at 21 K after a cooling period of 78 h is illustrated in Fig. 4. It is clear that this is a surface o-Ps, which means that $\tau_3=\tau_S\approx5$ ns and that $I_3\approx P_S$. This component is observable only in the specimen P1 and P2 because its intensity decreases with increasing particle size. The $P_S(T,t)$ vs $Q^{-1}(T,t)$ graph splits naturally into two distinct straight lines corresponding to the two particle sizes of P1 and P2. We may form one consistent set of data if we consider that the surface component is proportional to the specific surface S (cm^{-1}), which itself is probed by the initial amount of free o-Ps at RT, i.e., $P_S \propto S \propto P_3(0) \propto N_3(0)$. Thus we multiply the P_S data for the 0.3-μm sample by the ratio R of the total amount of o-Ps which is initially available, i.e., $R=[N_3(0)]_{0.05\ \mu m}/[N_3(0)]_{0.3\ \mu m}$. In this way we obtain the single linear relationship which is shown in Fig. 3

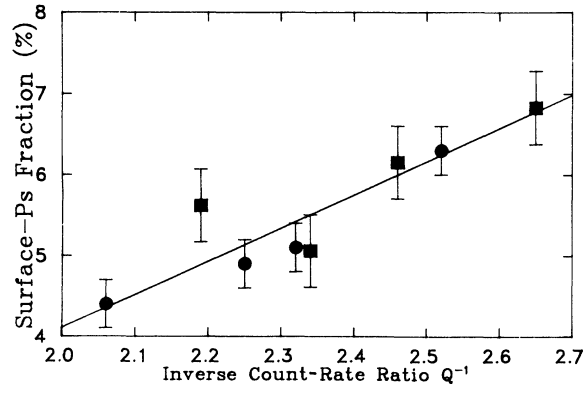

FIG. 3. The buildup of the surface orthopositronium state of ≈5 ns. For the powder of smallest particle size P1 the data (●) are as obtained from the lifetime spectra while the data for the particle size P2 (■) have been renormalized as explained in the text.

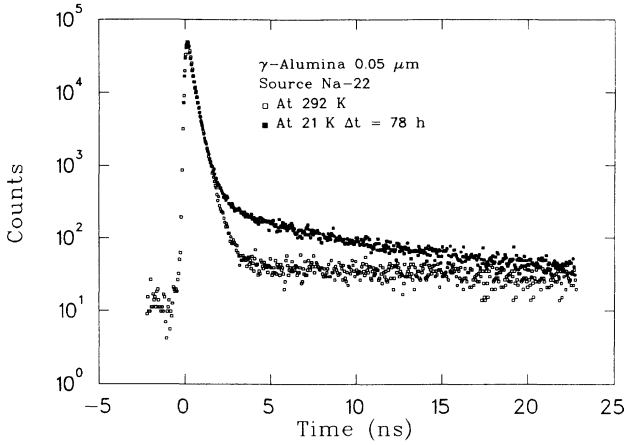

FIG. 4. Lifetime spectra illustrating the appearance of the surface orthopositronium component in powder P1 after cooling to 21 K for 78 h. The "constant" tail is caused by the free orthopositronium at ≈142 ns.

$$P_S(T,t)=k[Q^{-1}(T,t)-1] \quad \text{with } k=0.041\ , \tag{2}$$

where the P_S values for the 0.3-μm powder have been "normalized" at $P_S R$.

One might be inclined to conclude that the surface o-Ps is fed by the inhibition of the free interparticle o-Ps but this is certainly not so as the inhibition accounts only for a reduction of the volume o-Ps of 6.1%–5.8%, which means that a maximum of the order of 0.3% would be retained as surface positronium, however, we find surface o-Ps intensities up to 6%, which is 20 times higher. For the same consideration of relative intensities the possibility that the surface positronium be formed by capturing free positronium can be ruled out. Moreover a simple two-state trapping calculation shows that if a long-lived state λ_0 could be trapped into a much shorter surface state λ_S with a trapping rate κ_S, the effect would indeed be observed as a quenching of the long-lived component $\lambda_0 \rightarrow \lambda_0+\kappa_S$, but the shorter living state shows up as a component with intensity proportional to $\kappa_S/(\kappa_S+\lambda_0-\lambda_S)$. In this case the trapping constant κ_S contributes to the observed shortening λ_{qv} of the o-Ps component, i.e., $\kappa_S \leq \lambda_{qv}$. Considering the known values of the decay constants this component would have a negative intensity.

For the foregoing reasons the surface o-Ps is likely to be formed out of the preexistent surface positron state, which means that an increase of I_3 might be matched by a decrease of the surface positron state proposed by Brauer *et al.*, and which may contribute to the intensity of the second lifetime I_2. Unfortunately this second lifetime may contain more than one decay component and it has not been possible to relate the increase of I_3 to a clear matching decrease of the intensity of the second component I_2.

C. Three-quantum isotherms at 21 K versus source strength and type

Now that the lifetime experiments have revealed the fundamental processes such as free volume o-Ps inhibi-

tion and quenching and as surface o-Ps formation, we can use the three-quantum annihilation technique to study the accumulation of the defects which are responsible for these processes in some detail. As it is supposed that the hitherto observed effects are due to radiation-induced defects we obtained a number of three-quantum count rate isotherms at ≈ 25 K with different sources and source strengths, which are reproduced in Fig. 5. The data B and D correspond, respectively, to ^{68}Ge sources S2 and S1, the latter being approximately 1.6 times stronger than the former, which explains the stronger rate of defect formation.

Next we tried to increase the primary defect production by preparing a few electron sources of ^{204}Tl on Kapton foil to be inserted together with the positron source S2. The purpose is that the ^{204}Tl electrons which have an end-point energy of 763 keV are slowed down in the specimen in almost the same way as the energetic positrons with the production of an additional amount of defects, and thus we expect isotherms which descend more steeply than isotherm B. The experimental evidence is quite surprising; the addition of 5.5 μCi of ^{204}Tl, source S2+S3, results apparently in a decreased surface defect production (curve A). We might explain this effect by the assumption that the ^{204}Tl source creates an excess amount of a second bulk defect which traps or recombines our primary interstitial in its diffusional motion to the surface. Addition of a stronger 16.5-μCi ^{204}Tl source, however, inverts the trend to a seemingly "normal" increase of the surface defect production (source S2+S4, and curve C). When an extremely intense 38.5-μCi ^{204}Tl source is added (S2+S5) the isotherm, not shown in Fig. 5, fails to accuse a further accentuated effect and the whole isotherm remains situated in the zone between the data C and D. All these results for combined ^{68}Ge and ^{204}Tl sources indicate that at least two interacting defects are involved but that much more work will be needed to reach a good understanding of the processes. The isotherm with the strongest variation was obtained with a relatively weak ^{22}Na source S6, curve E, which was used for the detection of the surface intermediate-lifetime component of Sec. III B. From the foregoing we may safely conclude that the rate of surface defect production depends on the activity of the source but also on energy distribution of the electrons or positrons and that probably at least two interacting defects are produced.

D. Three-quantum isotherms versus temperature

Measuring the three-quantum isotherms of the 0.05-μm alumina powder P1 for a range of temperatures with the ^{68}Ge positron source S2 allows the study of the temperature dependency of the surface defect formation rate. Figure 6 shows the observed three-quantum isotherms represented as Q vs t for various temperatures T. The initial slope of these isotherms increase steadily with decreasing temperature and the general aspect of the curves suggests an analysis by a two-parameter model, i.e., a defect production rate, responsible for the decrease of Q, and a recombination or annealing rate which is responsible for the saturation tendency of Q for very long cooling times.

In order to be observable as surface defects in our fine powders the irradiation-induced defects, presumably interstitials, should diffuse outwards and ultimately be trapped at the surface. As irradiation proceeds with time more and more interstitials escape to the surface and the bulk accumulates an increasing concentration of vacancies, thus the vacancy-interstitial recombination rate per unit time increases and consequently the fraction of interstitials reaching the surface, or production rate, should decrease with time unless the vacancy-interstitial recombination rate is several orders of magnitude lower than the interstitial escape rate, which would mean that virtually all the produced interstititals are "sucked" to the surface. This possibility can be checked experimentally; when a particular source-powder combination is cycled

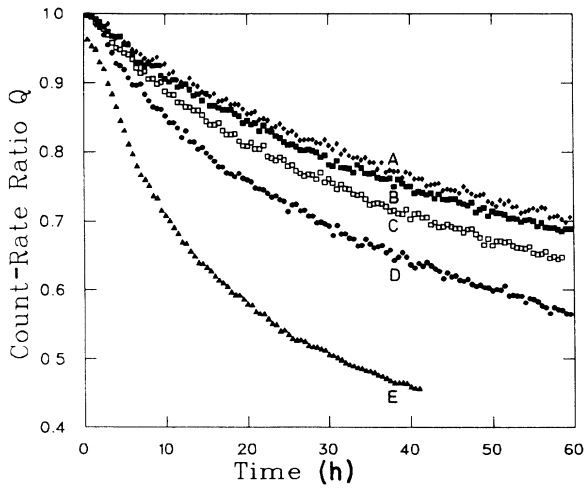

FIG. 5. Three-quantum count rate isotherms at 20–25 K in sample P1 for different sources and source strengths. Positron and electron sources used are, respectively, data A: (S2+S3), data B: (S2), data C: (S2+S4), data D: (S1), and data E: (S6).

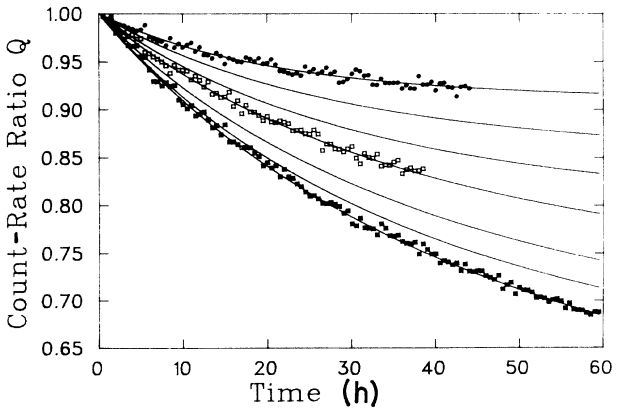

FIG. 6. Alumina powder of 0.05 μm mean diameter; reduction of the three-quantum count rate with time after cooling to temperature T with ^{68}Ge positron source S2. The curves from low to high correspond to the temperatures 25, 45, 65, 85, 95, 105, and 115 K. Some experimental data are omitted for the sake of clarity; the solid lines are the best fits of Eq. (3).

many times between RT and low temperatures only the surface defects may disappear at RT but the corresponding bulk vacancies and associated color centers are stable, which means that for a series of consecutive isotherms an increasing initial concentration of vacancies should induce a decreasing of the initial slope, i.e., $|(dQ/dt)_{j+1}| < |(dQ/dt)_j|$, where j is the cycle number.

In order to evaluate this possibility we have cycled the 0.05-μm powder and ^{22}Na-source combination five times between 40 K and RT, corresponding to a total cooling time of 200 h, and we have analyzed the five consecutive three-quantum isotherms; the obtained production rates, or initial slopes stayed constant within a statistical scatter of 4%. Thus we conclude that diffusion to the surface is dominant, that the interstitial-vacancy recombination is only of second order of magnitude and that the migration of the induced interstitials to the surface may be described by a time-independent creation rate.

E. Discussion

Let us first consider the fundamentals of formation of positronium and of radiation-induced interstitials in fine particles of oxide powders such as silica or alumina. When an amount of energetic positrons N is injected into dense material they may produce a great amount of displaced atoms or interstitials and their associated vacancies. Once the positron kinetic energy has fallen below the displacement threshold energy, thermalization will proceed through electron-positron scattering, by which a certain quantity of positronium can be formed which is alternatively explained by the Ore-gap concept or by the spur model. At high temperatures and in macrocrystalline material these interstitials eventually recombine with vacancies and thus the primary defect production by the positron may be safely ignored. In fine powdered material, however, these interstitials may migrate to the surface of the particles and emerge as surface defects. The bulk orthopositronium itself decays with a mean bulk decay constant $\lambda^B_{o\text{-Ps}}$ but also migrates to the surface and escapes into the interparticle space as hot free positronium. This free positronium collides with the surfaces and thus interacts with the surface defects. The bulk positrons decay with a decay constant λ^B and also migrate to the surface where they may escape as free positrons or where they may be trapped in a surface positron state or a surface positronium state. The parameters which we study here are the free o-Ps fraction $P_F = N_F/N$, its lifetime τ_F, the surface orthopositronium fraction P_S, its lifetime τ_S, and the total three-quantum yield N_3 produced from the natural decay branching of these two o-Ps states.

The ideal situation is encountered in low-density clean surface alumina where no appreciable amount of surface positronium has been found and where the zero-density extrapolated lifetime of the free o-Ps tends to the natural decay lifetime of 142 ns, i.e., $P_S \to 0$ and $\beta_F = \tau_F/\tau_0 \to 1$.

As a consequence of the foregoing observations (Secs. III A–III C) let us consider the situation where the surface contains a time- and temperature-dependent concentration $c(T,t)$ of defects which interact with the positron and the positronium. A first effect is the quenching of the free o-Ps, thus $\lambda_F = \lambda_0 + \lambda_{qv}$ where the quenching rate λ_{qv} is supposedly proportional to the defect concentration, i.e., $\lambda_{qv} = \mu c(T,t)$. The quenching efficiency μ depends on the frequency of collision with the particles and on the interaction time for each collision. These two factors depend on the effective positronium temperature and we may consider them as a constant for nonthermalized positronium. As a second effect the escape of o-Ps from the particles is inhibited or anti-inhibited, i.e., the free o-Ps fraction may decrease or increase. From the arguments of Sec. III A we conclude that the most probable mechanism for inhibition is also proportional to the surface defect concentration and we write $P_F(T,t) = P_F(0)[1 - k_1 c(T,t)]$, where k_1 is the inhibition constant for a particular surface defect, the inhibition is small, i.e., $k_1 c \ll 1$, and $P_F(0)$ is the free o-Ps fraction at zero induced surface defect density which can be obtained before irradiation or at high temperatures where the induced surface defects have disappeared. In the case of alumina all positron-active surface defects seem to be annealed at room temperature.

The third effect is the formation of a positroniumlike surface state by forming supplementary o-Ps from the existing surface positrons. Because the intensity of this surface orthopositronium state is zero in unirradiated samples and because it increases with irradiation time we consider its formation probability to be proportional to the surface defect concentration, and it has a decay constant $\lambda_S = (\lambda_0 + \lambda_{qs})$ where λ_{qs} is the quenching constant of the surface o-Ps. The possibility exists that the surface contains different types of defects and that each defect has its own quenching, inhibition, and surface-Ps forming constants but at the moment we will limit ourselves to a description with only one defect type. The three-quantum-annihilation count rate N_3 is calculated from the branched decay of all o-Ps, and from the natural decay into three quanta of all positron states,

$$N_3(T,t) \propto \beta_F P_F(T,t) + \beta_S P_S(T,t) + \tfrac{1}{372}[1 - P_F(T,t) - P_S(T,t)] \tag{3a}$$

with $\beta_F = \tau_F/\tau_0$ and $\beta_S = \tau_S/\tau_0$,

$$N_3(0) \propto P_F(0) + \tfrac{1}{372}[1 - P_F(0)] , \tag{3b}$$

where $N_3(0)$ is the count rate with a vanishing surface defect concentration which is obtained here simply by heating the sample to room temperature. Let us first consider the expected variation in each of the three right-hand terms of Eq. (3a); $P_F(0)$ can amount easily to 20–50 % in fine powders, although in our finest powder it is only 6% (see Sec. III A) and β_F varies from ≈ 1 to ≈ 0.5, thus the left-hand (free o-Ps) term varies from 6% to 3%. In the middle term $P_S(T,t)$ varies from 0 to $\approx 6\%$ (see Sec. III B) and the surface orthopositronium lifetime ratio β_S is taken constant at $\frac{5}{142} = 0.035$, thus the middle or surface o-Ps contribution varies from 0 to $\approx 0.21\%$. Finally the right-hand or free-positron term varies from 0.253% to 0.237%, i.e., a variation of only 0.015%. Thus we see that the variations of the three

terms in Eq. (3a) relate as 100:10:1 and that we may safely ignore the three-quantum variation due to the free positrons, and that in some cases even the surface *o*-Ps contribution can be ignored within experimental error.

A simplified form of Eqs. (3) is then

$$N_3(T,t) \propto \beta_F P_F(T,t) + \beta_S P_S(T,t) , \tag{3c}$$

$$N_3(0) \propto P_F(0) . \tag{3d}$$

These expressions depend on the surface defect concentration $c(T,t)$. This concentration is fed by the diffusion of the radiation-induced aluminium interstitials and thus it depends on temperature, source strength, source type, and energy distribution, and the particle mean diameter. For a given set of these parameters the surface defect formation rate will be independent of time as long as the vacancy-interstitial recombination rate can be ignored, which is the case for our isotherms (see Sec. III D). The extra surface aluminium atoms or ions may recombine or cluster, giving rise to a decrease of the Ps-quenching centers which can formally be described as an annealing. Nothing can be said *a priori* about the order of this annealing process, but for most of our isothermal three-quantum curves a first-order annealing term gives a good statistical fit. In a few cases it was clear that a first-order annealing term is an oversimplification, specially the isotherms which were obtained with combined ^{68}Ge-^{204}Tl sources. In the simplest case of first-order annealing the surface defects concentration is given by

$$c(T,t) = \frac{a(T)}{\nu(T)} (1 - e^{-\nu(T)t}) , \tag{4}$$

where $a(T)$ is the production rate and $\nu(T)$ the first-order annealing rate.

We easily find the expressions to be fitted to the experimental data:

$$Q(T,t) = \frac{N_3(T,t)}{N_3(0)} = \frac{1 - k_1 c(T,t)}{1 + a_1 c(T,t)} + a_2 c(T,t)$$

$$\text{with } a_1 = \mu\tau_0 \text{ and } a_2 = \frac{\beta_S k_2}{P_F(0)} , \tag{5a}$$

$$P_F(T,t) = P_F(0)[1 - k_1 c(T,t)]$$

$$= P_F(0)[1 - (k_1/\mu)\lambda_{qv}] , \tag{5b}$$

$$\lambda_F = \lambda_0 + \mu c(T,t) , \tag{5c}$$

$$P_S(T,t) = k_2 c(T,t) = (k_2/\mu)\lambda_{qv}$$

$$\text{with } \lambda_{qv} = (1/\beta_F - 1)\lambda_0 , \tag{5d}$$

$$\lambda_S = \lambda_0 + \lambda_{qs} . \tag{5e}$$

Now the experimental results from the foregoing sections can be quantified. The evolution of the long-lived lifetime, Sec. III A, is described by Eq. (5c) where we use Eq. (4) for the defect concentration. However, the lifetime values are subject to considerable statistical scatter and it is not reasonable to expect extracting very precise quantitative information from these. Therefore we approximated Eq. (4) by $c(T,t) \approx a(T)t$ and after fitting we obtain the product of the quenching efficiency times the surface defect creation rate $\mu a(77\text{ K}) = (3.0 \pm 0.1) \times 10^{-9}$ $(\text{ns})^{-1}\text{s}^{-1}$ for the source S7 and $\mu a(77\text{ K}) = (4.9 \pm 0.1) \times 10^{-9}$ $(\text{ns})^{-1}\text{s}^{-1}$ for source S8. Considering the uncertainty on the strengths of the two sources we may confirm numerically that the surface defect creation rate is proportional to the source strength.

The linear relation between the *o*-Ps fraction P_F and the quenching rate λ_{qv} which was found empirically (Fig. 2) is reproduced by the model Eq. (5b) where $k_1 = 0.17\mu\tau_0 = 0.17a_1$.

The occurrence of the surface positronium state from Sec. III B is described by Eq. (5d). However, the number of experimental P_S values (three for each specimen) and the statistical scatter do not allow a detailed verification of Eq. (5d) with a concentration represented by Eq. (4). Nevertheless when we consider the numerical orders we find that the empirical result of Eq. (2) has the same meaning; the count-rate-ratio first-order term is the quenching term, inhibition and surface three-quantum contribution being only corrections, and when neglecting these finer details Eq. (5a) reduces to $N_3(0)/N_3(T,t) - 1 \approx a_1 c(T,t)$, i.e., $P_S(T,t) \approx k a_1 c(T,t)$. From a comparison with Eq. (5d) we see that $k_2 \approx 0.041 a_1$ and thus $a_2 = \beta_S k_2 / P_F(0) \approx 0.024 a_1$ for the 0.05-μm alumina powder with ^{22}Na positron sources.

All the three-quantum versus time isotherms of Secs. III C and III D can be analyzed with the help of the model Eq. (5a) with Eq. (4) for the active surface defect concentration:

$$Q(T,t) = \frac{1 - (ak_1/\nu)(1 - e^{-\nu t})}{1 + (aa_1/\nu)(1 - e^{-\nu t})} + \frac{aa_2}{\nu}(1 - e^{-\nu t}) . \tag{6}$$

This expression contains only two fundamentally free parameters to be fitted to the experimental isotherms, i.e., the quenching efficiency times defect formation rate $\kappa = aa_1 = \mu\tau_0 a$ and the first-order annealing rate ν. We have found that the quality of fitting is relatively insensitive to the values of k_1 and a_2, which has the simple meaning that the three-quantum yield lost by the inhibition of free-volume positronium can always formally be compensated by an increased amount of surface positronium. It is therefore necessary to impose fixed values on k_1 and a_2 near to the numerical values which we obtained from the long- and intermediate-lifetime experiments, i.e., $k_1 \approx 0.17 a_1$ and $a_2 \approx 0.024 a_1$. Let us consider first the Q isotherms versus source type. The resulting values for κ and ν are represented in Table III. The isotherms B and D are obtained with ^{68}Ge sources of different strengths. From these two the weakest-source isotherm is very well fitted by the model function, while the stronger-source isotherm shows some diverging behavior during the first few points after cooling. Thus the first four points (at $\frac{1}{2}$ h per point) were not considered for the fitting procedure. The obtained annealing rates ν are nearly identical for both source strengths as is expected for a first-order recombination. The production times efficiency rates κ, however, are in a ratio of $3.96/2.48 = 1.6$, which is practically the same within experimental error as the source strength ratio $10.8/7.2 = 1.5$. We should note that we obtained the

same source strength dependency for the quenching of the free-orthopositronium lifetime with two ^{22}Na sources (see Sec. III A).

Finally all the isotherms of Fig. 6 were fitted by Eqs. (5a) and (4), resulting in reduced χ^2 values of 0.9–1.1; the temperature variation of the relevant parameters $\kappa(T)$ and $\nu(T)$ are represented in Fig. 7.

Both parameters are roughly constant at the lowest temperatures but at the temperatures higher than 70 K they seem to obey exponential laws $\kappa=\kappa_0 e^{-0.019T}$ and $\nu=\nu_0 e^{0.023T}$. This combination of decreasing formation rate and increasing annealing rate accounts for the fact that the experimental effect disappears for temperatures above 150 K. Whether the near equality of the production relaxation constant and the annealing relaxation constant is coincidental is a matter of further investigation.

The creation of a vacancy-interstitial pair by a primary knock on by a light particle is described by classical collision theory.[29] The original work of Arnold and Compton,[30] who studied the formation of an electron-irradiation-induced absorption band in Al_2O_3 at 204 nm was refined by Pells and Philips.[31,32] These authors observed the threshold energy for observable damage for temperatures between 320 and 1020 K. From the observation of optical absorption and luminescence of oxygen and aluminium vacancies they concluded that the threshold energies are widely different, i.e., 175±25 keV for the aluminium ion and 400±25 keV for the oxygen ion. The corresponding displacement energies are, respectively, 18 and 75 eV. This very low threshold energy for aluminium is the reason that a ^{22}Na source is very efficient in producing these interstitials. All existing data from the literature indicate that for electron irradiation in first approximation only the cation displacement has to be considered. Stathopoulos and Pells[33] have irradiated α-Al_2O_3 with 300-keV electrons in a high-voltage electron microscope, i.e., at an energy below the oxygen displacement threshold and they have observed the cation sublattice damage. They have observed that the Al interstitials are mobile and they precipitate between the basal planes. Around the same period Shikama and Pells[34] irradiated relatively thick plates of the same material with 1-MeV electrons at high temperatures ($\approx$1000 K). On subsequent examination at room temperature these authors observed among other effects that the Al^{3+} interstitials had precipitated into metallic aluminium clusters. The foregoing irradiations were all done at high temperatures where the high mobility of the formed interstitials allows

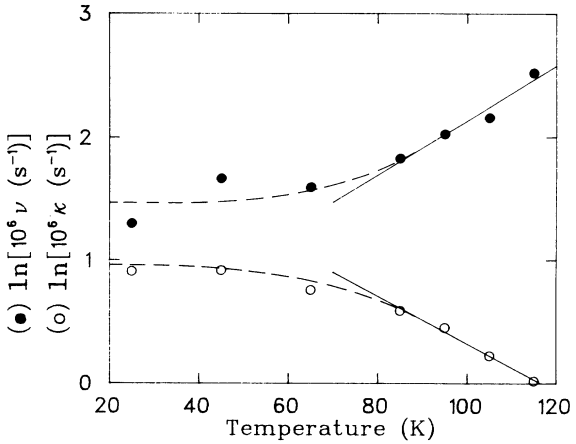

FIG. 7. Natural logarithm of the production parameter $10^6\kappa$ s^{-1} (○) and the annealing rate $10^6\nu$ s^{-1} (●) obtained from fitting (5) to the isotherm data of Fig. 6; the solid lines are linear regressions for $T>80$ K, and the dashed lines are simple visual representations of the evolution to constancy at lower temperatures.

the reorganization and the formation of extended defects, but low-temperature irradiation should allow the observation of the primary produced defects. Holmberg and Crawford[35] made ESR observations at 77 K of the centers which had been produced at 300 K by γ-ray irradiation. The effect of γ-ray irradiation in the 1-MeV region is similar to electron irradiation as γ rays interact with matter through the photoelectric and the Compton effect, both of which produce energetic electrons. These authors further could confirm the model given by Gamble *et al.*[36] in which the principal defect centers are one and two holes trapped on oxygen ions adjacent to Al^{3+} vacancies. In fine powdered material the aluminium interstitials migrate to the surface and may form metallic bridges between grains, resulting in a phenomenon known as low-temperature radiation sintering, a phenomenon which was described by Damask.[37]

It is clear that the positrons emitted by ^{68}Ge (end-point energy of 1890 keV) and ^{22}Na (end-point energy of 545 keV) as well as the electrons from ^{204}Tl (end-point energy of 763 keV) are efficient for defect generation by displacement of the aluminium cation. The high threshold for displacement of an oxygen anion precludes damage to the anion lattice by a ^{22}Na source but a ^{68}Ge positron source certainly creates interstitials of both kinds; in this case

TABLE III. Results of model function fitting to the three-quantum isotherms with different source types and source strengths.

Source	Isotherm (Fig. 5)	κ (10^{-6} s^{-1})	ν (10^{-6} s^{-1})	χ^2
S2+S3	*A*	2.17	3.0	0.98
S2	*B*	2.48	3.7	0.99
S2+S4	*C*	3.12	4.3	1.11
S1	*D*	3.96	4.1	1.24
S6	*E*	11.3	10.2	1.39
S2+S5	Not shown	3.78	7.0	1.00

aluminium and oxygen interstitials might recombine whereby a fraction of the migrating aluminium is trapped and no longer reaches the surface. Possibly this is the reason why apparently a ^{22}Na source is more efficient in quenching the free orthopositronium than the energetic ^{68}Ge source.

The diffusion of Al interstitials is fundamental to the creation of aluminium surface defects, and final states, either surface trapped or recombined, should be reached within experimental times. If $R \rightarrow \infty$ or $D_i \rightarrow 0$ the interstitials are effectively frozen in and can neither reach the surface nor recombine. The self-diffusion coefficient D_{Al} of aluminium in alumina was measured by Paladino and Kingery[38] in the temperature range 1670–1905 °C and was given as $D_{\mathrm{Al}} = 28e^{(-1.18\ \mathrm{eV})/k_B T}\ \mathrm{cm}^2/\mathrm{s}$. A similar Arrhenius relation was found for the oxygen self-diffusion coefficient by Oishi, Ando, and Suga,[39] who remarked that the experimental value D_{O} was somewhat dependent on the preparation of the surface but that a reasonable agreement with experiments was obtained with $D_{\mathrm{O}} = 562e^{(-6.88\ \mathrm{eV})/k_B T}\ \mathrm{cm}^2/\mathrm{s}$. If we extrapolate these expressions for D_{Al} and D_{O} to low temperatures, i.e., to 77 K the calculated diffusion constants become extremely small and the diffusion of any species to the surface is impossible. However, the self-diffusion is a vacancy-type diffusion, whereas the Al^{3+} interstitials move through the lattice by interstitial-type diffusion which may be many orders of magnitude higher. To our knowledge no data are available for interstitial diffusion in alumina but it seems logical that the very small Al^{3+} ion (0.39 Å) has a high mobility within a close-packed lattice formed by big O^{2-} ions (1.40 Å). A similar distinction between low-temperature interstitial migration and high-temperature vacancy-type migration occurs in the annealing of many irradiated pure metals, e.g., platinum; for this metal the high-temperature self-diffusion experiment yields a straight Arrhenius plot with an activation energy of 2.96 eV,[40] yet electron irradiation-induced interstitials recombine in five distinct stage-I steps at very low temperatures 11, 16, 21, 24, and 26 K, which have been identified as steps of close pair recovery (stages I_A, I_B, I_C), and free migration recovery (stages I_D, I_E) where the interstitials recombine with uncorrelated vacancies, other interstitials, or impurity atoms.[41] From all this it is sufficiently clear that the Al^{3+} interstitials indeed migrate to the surface of our powders even at 20 K and that the collected surface defects constitute the quenching agent for the free interparticle o-Ps. The observed o-Ps surface state is supposed to be a bound state of o-Ps to charged defects.

A last question is about the ionization state of the surface aluminum. Although the interstitials are supposedly Al^{3+} it is very unlikely that they conserve their triple charge upon migration to the surface because Al^{3+} has a Ne closed-shell configuration and offers no spin exchange mechanism whereby o-Ps could be quenched into two-quantum decay. Both the neutral Al atom ($3s^2 3p^1$) and the Al^{2+} ion ($3s^1$) have an unpaired electron capable of quenching the o-Ps by spin conversion to p-Ps followed by rapid two-quantum annihilation. On the basis of positron annihilation alone both charge states are acceptable. The neutral Al atom, upon surface migration may recombine into microscopic surface precipitates with metallic character and thus lose its paramagnetism and its Ps quenching ability. The recombination rate included in Eq. (5) is then associated with the surface migration and is consistent with the observed radiation sintering and metallic precipitation. In our opinion a neutral Al atom, however, could not explain the appearance of the surface o-Ps state at 5 ns. Because this state is absent in the unirradiated alumina we believe it to be an o-Ps bound to a surface charge, e.g., a $[\mathrm{Ps\text{-}Al}]^{x+}$ complex.

IV. CONCLUSIONS

There seem to exist six observable positron or positronium states in fine powdered alumina, i.e., one free-positron intrinsic bulk state at 140–160 ps, a surface positron state, and a bulk qPs state which have similar lifetimes and are mixed up to form a single experimental component at 360–430 ps, a state possibly associated with the structural vacancies in γ-alumina at ≈ 700 ps, and finally two orthopositronium states, i.e., a surface o-Ps state at 5 ns, and the interparticle free o-Ps state. Corresponding parapositronium states at 124 ps are too short to be distinguishable and are mixed up with the shortest positron lifetime. The existence of the surface orthopositronium state and the modifications to lifetime and intensity of the interparticle orthopositronium are directly connected to the radiation damage induced on the grain surface by the positron (or electron) source. The surface radiation damage is due to the migration to, and trapping onto, the surface, of bulk aluminum interstitials which are created by electron-atom collisions at electron (positron) energies above the known threshold energies.

The free o-Ps is quenched by surface defects, which results in a lowering of its lifetime from the theoretical free-space value of 142 ns to 100 ns or less. The combination of inhibition and quenching of the free o-Ps state (first-order-of magnitude term) and of the creation of a strongly quenched surface o-Ps term (second order of magnitude) is observed. The charge state of the extra surface aluminium atoms or ions is unknown.

[1]D. G. Costello, D. E. Grace, D. F. Herring, and J. Wm. McGowan, Phys. Rev. B **5**, 1433 (1972).

[2]A. P. Mills, in *Positron Annihilation,* edited by P. G. Coleman, S. C. Sharma, and L. M. Diana (North-Holland, Amsterdam, 1982), p. 121.

[3]R. Paulin and G. Ambrosino, J. Phys. (Paris) **29**, 263 (1968).

[4]S. M. Curry and A. L. Shawlow, Phys. Lett. **37A**, 5 (1971).

[5]A. P. Mills, Jr., E. D. Shaw, R. J. Chichester, and D. M. Zuckerman, Phys. Rev. B **40**, 2045 (1989).

[6]N. Mbungu-Tsumbu, C. Dauwe, M. D. Diatezua, L. Mbosei, and K. Motoko, Appl. Phys. A **48**, 343 (1989).

[7]M. Eldrup, A. Vehanen, P. J. Schultz, and K. G. Lynn, Phys. Rev. Lett. **51**, 2007 (1983).

[8]S. Berko, M. Haghgooie, and J. J. Mader, Phys. Lett. **63A**, 335

(1977).
[9]M. Kakimoto, T. Hyodo, and K. Fujiwara, in *Positron Annihilation,* edited by P. C. Jain, R. M. Singru, and K. P. Gopinathan (World Scientific, Singapore, 1985), p. 776.
[10]J. Kasai and K. Fujiwara, J. Phys. Soc. Jpn. **51**, 3077 (1982).
[11]K. Fujiwara, in *Positron annihilation* (Ref. 2), p. 615.
[12]C. Dauwe, unpublished results.
[13]D. D. Uphadhyaya, R. V. Muraleedharan, B. D. Sharma, and K. G. Prasasad, Philos. Mag. A **45**, 509 (1982).
[14]Y. C. Jean, K. Venkateswaran, E. Parsai, and K. L. Cheng, Appl. Phys. A **35**, 169 (1984).
[15]M. Forster, J. N. Mundy, and H. E. Schaefer, in *Positron Annihilation,* edited by L. Dorikens-Vanpraet, M. Dorikens, and D. Segers (World Scientific, Singapore, 1989), p. 833.
[16]W. Brandt, Appl. Phys. **5**, 1 (1974).
[17]G. W. Ford, L. M. Sander, and T. A. Witten, Phys. Rev. Lett. **36**, 1269 (1976).
[18]M. Kakimoto, T. Hyodo, T. Chiba, T. Akahane, and T. B. Chang, J. Phys. B **20**, L107 (1987).
[19]S. Y. Chuang and S. J. Tao, Appl. Phys. **3**, 199 (1974).
[20]R. F. Kiefl and D. R. Harshman, Phys. Lett. **98A**, 447 (1983).
[21]P. C. Rice-Evans, M. Mousavi-Madani, K. U. Rao, D. T. Briton, and B. P. Cowan, Phys. Rev. B **34**, 6117 (1986).
[22]P. C. Rice-Evans and M. Mousavi-Madani, Phys. Lett. A **122**, 187 (1987).
[23]R. F. Kiefl, J. B. Warren, Chris. J. Oram, G. M. Marshall, J. H. Brewer, D. R. Harsman, and C. W. Clawson, Phys. Rev. B **26**, 2432 (1982).
[24]C. Dauwe, Appl. Phys. **24**, 279 (1981).
[25]J. B. Peri, J. Phys. Chem. **69**, 220 (1965).
[26]D. W. Gidley, K. A. Marko, and A. Rich, Phys. Rev. Lett. **36**, 395 (1976).
[27]C. Dauwe (unpublished).
[28]G. Brauer, F. Kerbe, Zs. Kajcsos, and A. Ashry, Phys. Status Solidi A **84**, 451 (1984).
[29]M. Kiritani Progress, in *The Study of Point Defects,* edited by Masao Doyama and Sho Yoshida (University of Tokyo Press, Tokyo, 1977).
[30]G. W. Arnold and W. D. Compton, Discuss Faraday Soc. **31**, 130 (1961).
[31]G. P. Pells and D. C. Philips, J. Nucl. Mater. **80**, 207 (1979).
[32]G. P. Pells and D. C. Philips, J. Nucl. Mater. **80**, 215 (1979).
[33]A. Y. Stathopoulos and G. P. Pells, Philos. Mag. A **47**, 381 (1983).
[34]T. Shikama and G. P. Pells, Philos. Mag. A **47**, 369 (1983).
[35]G. E. Holmberg and J. H. Crawford, Solid State Commun. **20**, 183 (1976).
[36]F. T. Gamble, R. H. Bartram, C. G. Young, O. R. Gilliam, and P. W. Levy, Phys. Rev. **134**, A589 (1964).
[37]A. C. Damask, Radiat. Effects **1**, 95 (1969).
[38]A. E. Paladino and W. D. Kingery, J. Chem. Phys. **37**, 957 (1962).
[39]Y. Oishi, K. Ando, and N. Suga, J. Am. Ceram. Soc. **66**, 130 (1983).
[40]N. L. Peterson, J. Nucl. Mater. **69&70**, 3 (1978).
[41]W. Shilling and K. Sonnenberg, J. Phys. F **3**, 322 (1973).